Structural and Catalytic Properties of the Expressed and Purified NAD(H)- and NADP(H)-Binding Domains of Proton-Pumping Transhydrogenase from *Escherichia coli*†

Ola Fjellström, Carina Johansson, and Jan Rydström*

Department of Biochemistry and Biophysics, Göteborg University and Chalmers University of Technology, S-413 90 Göteborg, Sweden

Received April 24, 1997; Revised Manuscript Received July 15, 1997⊗

ABSTRACT: Proton-pumping nicotinamide nucleotide transhydrogenase from *Escherichia coli* contains three domains: the hydrophilic domains I and III harbor the binding sites for NAD(H) and NADP(H), respectively, and domain II represents the membrane-spanning region. Proton translocation involves primarily domain II but possibly also domain III, which contains the essential βAsp392 residue. In the present investigation, the major portions of domain I (EcTHSα1 and EcTHSα2) and domain III (EcTHSβ1) were overexpressed in *E. coli* and purified therefrom. EcTHSβ1 was purified mainly in its holoform containing approximately 95% $NADP^+$ and 5% NADPH. When combined, EcTHSα1/EcTHSα2 and EcTHSβ1 were catalytically active, indicating native-like structures. Due to the lack of structural information and its possible role in proton pumping, EcTHSβ1 was primarily characterized. Substrate-binding characteristics and conformational changes were investigated by fluorescence and CD. Fluorescence arising from the single βTrp415 of EcTHSβ1 was quenched upon binding of NADPH by resonance energy transfer, an effect that provides an important tool for investigating substrate interactions with this domain and the determination of K_d values. The apparent relative binding affinity for NADPH was found to be about 50 times higher than that for $NADP^+$. Circular dichroism was used to estimate secondary structure content and for conformational analysis of EcTHSβ1 in the absence and presence of added substrates at various temperatures. Results show that domain III complexed with NADPH or $NADP^+$ adopts different conformations. Isoelectric focusing and native gel electrophoresis experiments support this finding. It is proposed that these structural differences play a central role in a conformationally-driven proton pump mechanism of the intact enzyme.

Nicotinamide nucleotide transhydrogenases (EC 1.6.1.1) catalyze the reduction of $NADP^+$ by NADH and a concomitant translocation of *n* protons according to the reaction:

$$n\mathrm{H^+_{out}} + \mathrm{NADH} + \mathrm{NADP^+} \rightleftharpoons n\mathrm{H^+_{in}} + \mathrm{NAD^+} + \mathrm{NADPH}$$

It is generally concluded that the value of "*n*" is 1. Transhydrogenases from several different sources have been isolated and reconstituted in liposomes, and their kinetic and functional properties have been characterized. At present, 10 transhydrogenase genes have been cloned. All transhydrogenases are homologues, the overall amino acid sequence identity is about 23%, and they are generally homodimers. The major domains contain the two proposed substrate-binding sites, one for NAD(H) (domain I) and one for NADP(H) (domain III), and the predicted 10−14 transmembrane α-helices presumably forming a proton-conducting structure (domain II) (Figure 1). Transhydrogenases are conformationally-driven proton pumps where the conformational states are thought to be primarily regulated by the ligands/substrates occupying the NADP(H) site, with the NAD(H) site providing reducing equivalents for $NADP^+$ reduction [for reviews, see Olausson et al. (1995) and Jackson (1991)].

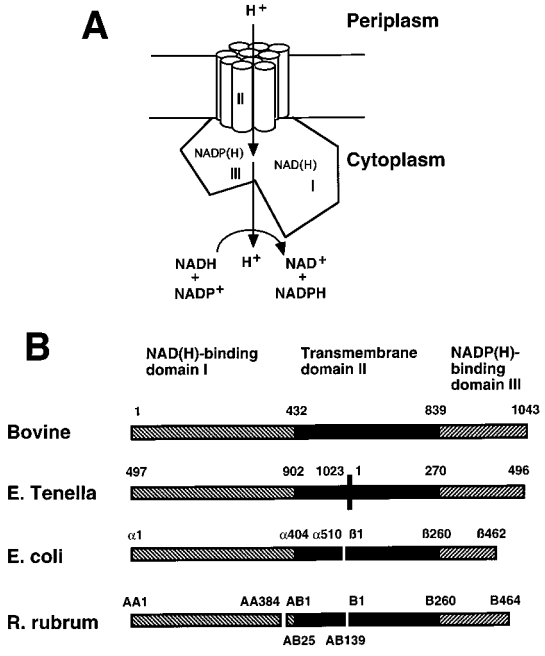

FIGURE 1: Schematic representation of the transhydrogenase structure (A) and domain organization (B) in various species. The basic structural features are shown in (A). In (B), the domain organizations at the primary structure level of four representative classes of transhydrogenases (*E. coli*, bovine, *R. rubrum*, and *E. tenella*) are compared.

The argument that domain II is directly involved in proton translocation is mainly based on the importance of βHis91

† This work was supported by the Swedish Natural Sciences Research Council and the Lawsky Foundation.

* To whom correspondence should be addressed.

⊗ Abstract published in *Advance ACS Abstracts,* September 1, 1997.

S0006-2960(97)00958-6 CCC: $14.00

for proton pumping by *E. coli* transhydrogenase (Olausson et al., 1995; Holmberg et al., 1994; Glavas et al., 1995). The latter residue is located in the predicted helix 7 of this enzyme and constitutes the only protonable residue identified in the predicted membrane structure (Holmberg et al., 1994). There is also an established functional coupling between βHis91 and the NADP(H) site. The pronounced conformational change that normally accompanies binding of NADP(H), and which leads to an increased sensitivity to trypsin, is maintained in the absence of added NADP(H) in the βH91K mutant (Glavas et al., 1995). It was subsequently shown that this mutant transhydrogenase contained bound NADP(H), and catalyzed a cyclic reduction of 3-acetylpyridine−NAD^+ ($AcPyAD^+$)[1] by NADH mediated by the bound NADP(H) (Glavas et al., 1995). In addition, the aspartic acid residue βAsp392 in domain III was found to be essential for catalytic activity and proton pumping (Meuller et al., 1996). Thus, it was proposed that the βHis91 and βAsp392 residues constitute parts of the proton-conducting pathway (Meuller et al., 1996).

Following the cloning and characterization of the soluble domain I of *R. rubrum* transhydrogenase (Williams et al., 1994; Yamaguchi & Hatefi, 1994), this domain as well as a somewhat smaller part of domain I from the *E. coli* enzyme (Diggle et al., 1995a,b; Yamaguchi & Hatefi, 1997) have both been expressed in *E. coli* and found to be catalytically active. Particularly the NAD(H)-binding site of domain I has been characterized extensively (Diggle et al., 1995a; Bizouarn et al., 1996b), e.g., with regard to a mobile loop that is assumed to be involved in the binding of NAD(H) (Bizouarn et al., 1996a; Diggle et al., 1996b). Domain III has so far been less well characterized as such, especially that from *E. coli*, despite the fact that this domain may contain a residue directly involved in proton translocation. However, domains III from both beef heart (Yamaguchi & Hatefi, 1995, 1997) and *R. rubrum* (Diggle et al., 1996a; Yamaguchi & Hatefi, 1997) have been expressed and isolated. They were found to be monomeric, contain stoichiometrically bound NADP(H), and catalyze a rapid cyclic reduction of $AcPyAD^+$ by NADH mediated by the bound NADP(H) in the presence of *R. rubrum* domain I.

The present paper describes the overexpression of active domains I and III of *E. coli* transhydrogenase in the same host and their purification and spectroscopic properties, with emphasis on domain III. CD measurements and absorption spectroscopy reveal helical content and bound NADP(H), respectively. The intrinsic fluorescence of domain III due to the single βTrp415 residue in the vicinity of the NADP(H) site is quenched by NADPH and provides an excellent probe for binding of NADPH to the enzyme and structural stability.

MATERIALS AND METHODS

Materials. $NADP^+$, NADPH, $NADP^+$, and $AcPyAD^+$ were purchased from Sigma Chemical Co., and NADH was from Biomol (Hamburg, GmbH). Other biochemicals were of analytical grade and purchased from Sigma or Boehringer-Mannheim.

Bacterial Strains and Plasmids. The *pnt* gene introduced in the pUC13 plasmid, giving a construct denoted pDC21 (Clarke & Bragg, 1985), was transformed into *E. coli* K12 strain TG1. Alternatively, the *pnt* gene was introduced in the pGEM-7Zf(+) plasmid, resulting in the construct denoted pSA2 (Ahmad et al., 1992).

Construction and Expression of the EcTHSα1 and EcTHSα2 Genes. A six residue long N-terminal histidine tag was introduced by insertional mutagenesis into transhydrogenase expressed from pDC21 by an overlap extension PCR technique. The primers used in the mutagenesis were constructed to insert $(CACCAT)_3GGT$ between the start codon and αArg2. A glycine after the six histidines was introduced to make the His-tag more flexible and to introduce an *Nco*I site. In addition, the codon for αArg2 was changed from CGA to CGT which is a more frequently used codon in *E. coli*. The wild-type sequence between *Pst*I and *Xho*I was replaced with the PCR-produced fragment containing the insertion. The new construct, called pNHis, was sequenced over the replaced region with one T to G base substitution at a position 38 bases upstream of the start codon.

The EcTHSα1 gene was constructed from pNHis by restriction enzyme cleavage with *Nae*I and *Sma*I, both yielding blunt ends. The cut vector was separated from the fragment on an agarose gel and electroeluted onto DEAE membranes. Subsequent blunt end ligation yielded the final product. EcTHSα1 includes residues αMet1−αPro369 plus a 13 residue long non-native C-terminal tail with the sequence GELEFTGRRFTTS. The plasmid containing insert was transformed into TG1 *E. coli* cells by electroporation using 1 mm cuvettes (BTX Inc., USA) and a voltage setting of 1.2 kV. Plasmid DNA was isolated using the QIAprep Spin Plasmid Miniprep Kit (Qiagen, GmbH, Germany).

In the case of EcTHSα2, which includes residues αMet1−αLys394, the pNHis plasmid was used as template for PCR amplification. Forward primer was GCT GCT GCG GAT CCT TAT TTT TCC TCA GTT TTC ACT TC (*Bam*HI recognition site underlined). Reverse primer was M13 universal Rp. The PCR product was purified with the QIAquick PCR purification Kit (Qiagen, GmbH, Germany), and the resulting fragment and the intact vector were cut with *Bam*HI and *Nco*I. The cut vector and fragment were purified with the Qiaex II Agarose Gel Extraction Kit (Qiagen, GmbH, Germany), and the new fragment was inserted by ligation. The final construct was transformed into TG1 *E. coli* cells by electroporation as described above.

Purification of EcTHSα1 and EcTHSα2. TG1 *E. coli* cells containing the modified pNHis plasmid were grown at 37 °C for about 16 h, harvested by centrifugation at 4000 rpm for 50 min at a temperature of 4 °C, using a 4.2 rotor in a Beckman J6-MC centrifuge. Cells were resuspended in buffer A [10 mM sodium phospate (pH 6.2), 1.0 mM DTT], using a volume of 5 mL of buffer/g of wet cells. The cell suspension was homogenized and then applied to a French press with the pressure set at 5−6 bar. Cell debris and membranes were removed by ultracentrifugation at 40 000 rpm for 2.5 h at a temperature of 4 °C, using either a Ti45 or a Ti70 rotor in a Beckman L-60 ultracentrifuge. The supernatant was applied to a DE32 anion-exchange column equilibrated with buffer A. The column was washed with buffer A containing 70 mM NaCl, and the sample was eluted with buffer A containing 300 mM NaCl. Fractions with EcTHSα1 were pooled and concentrated by dialysis against

[1] Abbreviations: DTT, dithiothreitol; $AcPyAD^+$, 3-acetylpyridine−NAD^+; *R. rubrum*, *Rhodospirillum rubrum*; *E. tenella*, *Eimeria tenella*; *E. acervulina*, *Eimeria acervulina*; *E. histolytica*, *Entamoeba histolytica*.

polyethylene glycol 20M to about 80 mL. A sodium phosphate (pH 6.2) solution containing 4 M NaCl was added to the sample to give a solution compatible with buffer B [10 mM sodium phosphate (pH 6.2), 0.8 M NaCl]. The next step involved immobilized metal chelate affinity chromatography (IMAC). The sample was applied to a $ZnSO_4$-loaded Chelating Superose column from Pharmacia Biotech, equilibrated with buffer B. Impurities were removed by washing with buffer B containing 1.8 M NH_4Cl. EcTHSα1 was eluted with an imidazole gradient (0−50 mM imidazole in 80 mL of buffer B). Pooled fractions containing EcTHSα1 were concentrated to approximately 15 mL by a Centriprep-10 concentrator (Amicon Inc., USA), followed by extensive dialysis against 10 mM sodium phosphate (pH 6.2) and 1 mM DTT.

EcTHSα2 was purified in a similar manner as described above for EcTHSα1, with the exception that EcTHSα2 was eluted by an NH_4Cl gradient (0−1.5 M NH_4Cl in 50 mL of buffer B) in the IMAC purification step.

Construction of the EcTHSβ1 Gene. A modified pET8c plasmid was chosen as expression vector. Modifications included insertion of an N-terminal His-hexamer, removal of the *Nco*I recognition site, and creation of an *Xho*I site. C-terminally, a *Mlu*I recognition sequence had been introduced as a unique cloning site. These modifications were performed by Dr. Kolmerer at EMBL (Heidelberg, Germany), and the plasmid was kindly given to us.

The pSA2 plasmid was used as template for PCR amplification of the fragment corresponding to residues βGln286−βLeu462. Forward primer was TTT CTC GAG CCA GGA AGT GGG TGA GCA C (*Xho*I recognition site underlined). Reverse primer was TTT ACG CGT TAC AGA GCT TTC AGG ATT (*Mlu*I recognition site underlined). The PCR product was purified with the QIAquick PCR purification Kit, and the resulting fragment and the intact vector were cut with *Xho*I and *Mlu*I. The cut vector was purified with agarose gel electrophoresis followed by extraction from the gel using a JETsorb DNA extraction kit (Genomed, Germany), and the fragment was inserted by ligation. The new construct was transformed into BL21-(DE3) *E. coli* cells by electroporation as described above.

Purification of EcTHSβ1. BL21(DE3) *E. coli* cells containing the pET8c plasmid with insert were grown in minimal media (*Current Protocols in Molecular Biology*, Wiley, New York). At an OD_{600} of 1.3, protein expression was induced by adding IPTG to a final concentration of 0.4 mM in the medium; 6 h after IPTG addition, cells were harvested by centrifugation at 7000 rpm for 10 min at a temperature of 4 °C, using a Beckman J2-MC centrifuge and a JA10 rotor. Cells were disrupted by passage through an X-press (AB Biox, Göteborg, Sweden), and resuspended in buffer A [50 mM sodium phosphate (pH 8.0), 0.8 M NaCl, and 7 mM imidazole]. DNase was added, and cells were sonicated for 3 × 1 min (5 s pulses) using a Branson sonicator, disintegrator B-12, at a power setting of 5−6. Unbroken cells were removed by centrifugation at 10 000 rpm for 10 min at a temperature of 4 °C, using a Beckman JA20 rotor. Cell debris and membranes were removed by ultracentrifugation at 40 000 rpm for 2 h at a temperature of 4 °C, using a Beckman Ti70 rotor. The supernatant was applied to a Ni-NTA column (Qiagen, GmbH, Germany), equilibrated with buffer A. Washing was performed with buffer B containing 50 mM sodium phosphate (pH 8.0), 0.1 M NaCl, and 7 mM imidazole, and protein was eluted in an imidazole gradient (7−200 mM imidazole in 65 mL of buffer B). Fractions containing EcTHSβ1 were pooled and concentrated using Filtron Macrosep 3K tubes (Pall Filtron. Corp., USA) to a volume of about 4 mL. The sample was applied to a Superdex G75 size exclusion column from Pharmacia Biotech equilibrated with a 10 mM sodium phosphate buffer (pH 6.0) containing 0.1 M NaCl.

Catalytic Activity. Catalytic activities of domains I and III, separately and mixed together, were measured by following the reduction of $AcPyAD^+$ spectrophotometrically at 375−455 nm in a Schimadzu UV-3000, using the absorption coefficient 6100 mM^{-1} cm^{-1} (Palmer & Jackson, 1992). Medium contained 25 mM sodium phosphate buffer (pH 7.1) unless otherwise specified. Other conditions for the cyclic reduction of $AcPyAD^+$ by NADH in the presence of NADP(H), and the normal reverse reaction (reduction of $AcPyAD^+$ by NADPH), were as described (Zhang et al., 1997).

CD Measurements. The purified EcTHSα1 and EcTHSβ1 proteins were extensively dialyzed against 0.5 mM sodium phospate (pH 7.0). Concentrations of the samples were adjusted so that the total absorbance at 190 nm was within the range 0.8−1.0 using a 1 mm cuvette. Protein concentration was accurately determined spectrophotometrically on a Cary 4 UV−visible spectrophotometer by measuring the absorbance at 280 nm in the presence of 6 M urea, using the extinction coefficient 5690 M^{-1} cm^{-1} for tryptophan, and 1280 M^{-1} cm^{-1} for tyrosine (Johnson, 1990).

The CD spectra were recorded on a JASCO J-720 spectropolarimeter. Spectra for structure determination, and for thermal denaturation studies (values within parentheses), were recorded with the following instrumental settings: bandwidth, 2 nm (2 nm); slit width, auto (auto); response, 1 s (1 s); start λ, 260 nm (260 nm); end λ, 185 nm (200 nm); scan speed, 10 nm s^{-1} (50 nm s^{-1}); step resolution, 0.5 nm (0.5 nm); accumulation, 8 (8); temperature, ambient (variable). A 1 mm cell was used, and the compartment was constantly purged with nitrogen to minimize the absorption by oxygen. Calculation of secondary structure was based on the method developed by Hennessey and Johnson (1981), later modified by Weisberg (1985). Azurin and plastocyanin had previously been added to the basis set of proteins used in the calculations (Wittung et al., 1994). To minimize evaporation in the thermal denaturation experiments, 100 μL of mineral oil was added. Equilibration for 10 min was allowed at each temperature. CD data were expressed as differential absorption coefficients ($\Delta\epsilon = \epsilon_l - \epsilon_r$) per amino acid residue, based on 389 and 186 residues for EcTHSα1 and EcTHSβ1, respectively.

Fluorescence Measurements. Fluorescence spectra were recorded on a SPEX Model FL1T1 τ2 spectrofluorometer. A cuvette with 10 × 10 mm cross section was used. Excitation and emission slit widths were 3.5 nm if not stated otherwise. Primary inner filter effects were corrected for according to the equation: $I^{em}_{corr} = I^{em}_{obs} \times 10^{D(\lambda_{ex})l_p}$ (Kubista et al., 1994). The extinction coefficients used for $NADP^+$ and NADPH at 280 nm were 3960 and 3427 M^{-1} cm^{-1}, respectively. The instrumental l_p factor (distance from the point inside the cell at which luminescence is observed to the entry cell wall) was determined to be 0.507 cm. The secondary inner filter effect due to NADPH absorbance at 339 nm was only approximately corrected for by applying

Table 1: Activity Analysis of the Purified Soluble Domains EcTHSβ1, EcTHSα1, and EcTHSα2[a]

reaction	activity [nmol min^{-1} (mg of EcTHSβ1)$^{-1}$]	activity [nmol min^{-1} (mg of EcTHSα1)$^{-1}$]	activity [nmol min^{-1} (mg of EcTHSα2)$^{-1}$]
reverse reaction			
EcTHSα1 + EcTHSβ1	27	2	
EcTHSα1 + saturating EcTHSβ1	29	12	
EcTHSα1 + saturating EcTHSβ1, pH 5.7	80	33	
EcTHSα2 + EcTHSβ1	42		4
EcTHSα2 + saturating EcTHSβ1	25		14
EcTHSα2 + saturating EcTHSβ1, pH 5.7	67		37
cyclic reaction			
EcTHSα1 + EcTHSβ1	23	2	
EcTHSα1 + saturating EcTHSβ1	14	7	
EcTHSα1 + saturating EcTHSβ1, pH 5.7	72	36	
EcTHSα2 + EcTHSβ1	25		2
EcTHSα2 + saturating EcTHSβ1	21		10
EcTHSα2 + saturating EcTHSβ1, pH 5.7	130		59

[a] Saturation of EcTHSβ1 to either EcTHSα1 or EcTHSα2 was achieved by addition of EcTHSβ1 to the same reaction mixture. Similarly, to analyze the pH dependence, addition of acid was titrated into the same solution. Therefore, the initial substrate concentration in each series of measurements involving EcTHSβ1 and EcTHSα1 was 170 μM, and approximately 125 μM substrate was present in the final measurement, e.g., for EcTHSα1 + saturating EcTHSβ1 at pH 5.7. The corresponding concentrations in the measurements involving EcTHSα2 + EcTHSβ1 were approximately 10% higher. The concentration of both EcTHSα1 and EcTHSα2 was 0.18 mg mL^{-1} in all experiments. Initial EcTHSβ1 concentration was 0.018 mg mL^{-1}, and 0.08 mg mL^{-1} at saturating concentration. Unless otherwise indicated, the pH was 7.1.

the same equation as for the primary inner filter effect, now using the extinction coefficient 6200 M^{-1} cm^{-1}. The medium contained 25 mM sodium phosphate (pH 7.1), and the temperature was maintained at 20 °C. For binding studies, 15 min was allowed for equilibrium to be reached after each addition of NADPH before the intensity at 339 nm was recorded for 5 s. This procedure minimized the light-induced background decrease in quantum yield. It was assumed that $NADP^+$ and NADPH competed for the same binding site and that $NADP^+$ binding was strong; therefore, binding experiments were performed using at least a 10-fold molar excess of $NADP^+$ to EcTHSβ1, so that data could be analyzed analogous to competitive inhibition data. To minimize the complications due to inner filter effects, binding curves were only analyzed for NADPH concentrations up to about 2.5 μM.

Gel Filtration. A 25 mM sodium phosphate buffer (pH 7.1) containing 0.1 M NaCl was used. For analysis of EcTHSα1 and EcTHSα2+EcTHSβ1, Sephacryl S300 resin (Pharmacia, Uppsala, Sweden) was chosen, and for analysis of only EcTHSβ1, Superdex G75 (Pharmacia) was used. The columns were calibrated with Blue Dextran, bovine serum albumin, ovalbumin, carbonic anhydrase, and cytochrome *c* for subsequent molecular weight determinations.

Determination of Protein Concentration. Protein concentration was routinely determined optically, using the extinction coefficients for tryptophan and tyrosine as above, yielding $\epsilon_{EcTHS\alpha1} = 23\,470$ M^{-1} cm^{-1} and $\epsilon_{EcTHS\alpha2} = 10\,810$ M^{-1} cm^{-1}. The modified Lowry method developed by Peterson (1977) and the bicinchoninic acid assay were performed as complements, both with bovine serum albumin as standard.

Gel Electrophoresis. Isoelectric focusing, native gel electrophoresis, and SDS−PAGE were routinely performed with the Pharmacia LKB PhastSystem. Gels and buffer strips were purchased from Pharmacia Biotech, Uppsala, Sweden. The Laemmli protocol (Laemmli, 1970) was followed for complementary SDS−PAGE.

RESULTS

Expression and Purification of EcTHSα1, EcTHSα2, and EcTHSβ1. Expression and purification of the domain I constructs, EcTHSα1 and EcTHSα2, and the domain III construct, EcTHSβ1, were performed as described under Materials and Methods. In each case, approximately 3−10 mg of recombinant protein per liter of culture was obtained, with a purity greater than 90% as judged from SDS−PAGE gels (Figure 2). The theoretical molecular weights of EcTHSα1, EcTHSα2, and EcTHSβ1 were 41.6K, 42.8K, and 20.4K, respectively. The apparent molecular weight of EcTHSβ1 as judged from Figure 2 was approximately 29K. Also, SDS−PAGE using a 10% running gel and a 4% stacking gel, both containing 3 M urea, was run, but no mobility shift from the 29K position was detected (not shown). At present, the reason for the odd mobility of the soluble β subunit remains unknown.

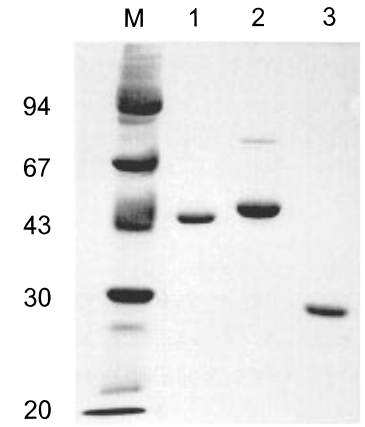

FIGURE 2: SDS−PAGE representation of the purified protein domains EcTHSα1, EcTHSα2, and EcTHSβ1. M denotes low molecular weight markers; lane 1, purified EcTHSα1 (1.5 μg); lane 2, purified EcTHSα2 (1.5 μg); lane 3, purified EcTHSβ1 (1.5 μg). The purification procedure is described under Materials and Methods. SDS−PAGE was performed according to Laemmli (1970) using a 12% polyacrylamide gel.

Catalytic Properties. Table 1 summarizes the results from the activity measurements. The data presented indicate that both the combinations EcTHSβ1+EcTHα1 and EcTHSβ1+EcTHSα2 were catalytically active, and both α domains displayed about equal catalytic potency. EcTHSα2 alone catalyzed low reverse transhydrogenase and cyclic activities, whereas EcTHSα1 and EcTHSβ1 alone were inactive (not

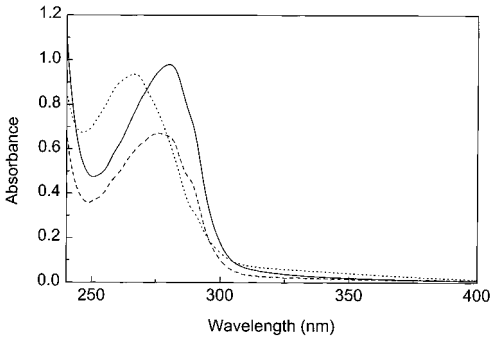

FIGURE 3: Optical spectra of EcTHSα1, EcTHSα2, and EcTHSβ1. The dashed line represents EcTHSα1 (1.2 mg/mL), the solid line EcTHSα2 (1.7 mg/mL), and the dotted line EcTHSβ1 (1.2 mg/mL). The level of purity was the same as that shown in Figure 2.

shown). The maximal rates of the reverse transhydrogenation reaction (reduction of $AcPyAD^+$ by NADPH) and of the cyclic reaction [reduction of $AcPyAD^+$ by NADH in the presence of bound NADP(H); Glavas et al., 1995] for the reconstituted systems were 67 and 130 nmol min^{-1} (mg of EcTHSβ1)$^{-1}$, respectively. It may also be seen from Table 1 that the rates for the normal reverse reactions were increased about 3-fold, and for the cyclic reaction about 6-fold, as the pH was lowered from 7.1 to 5.7. Turnover numbers for EcTHSβ1, in mixtures of EcTHSβ1 and EcTHSα2 at pH 7.1 and pH 5.7, were approximately 0.009 and 0.023 s^{-1} for the normal reverse reaction, and 0.007 and 0.044 s^{-1} for the cyclic reaction, respectively.

Molecular Properties of EcTHSα1 and EcTHSβ1. Gel exclusion chromatography was performed as described under Materials and Methods. The results revealed that EcTHSα1 was dimeric, whereas EcTHSβ1 was monomeric both in the absence and in the presence of 15 μM NADP(H) (not shown). These findings agree with what has previously been observed for the counterparts of these domains in bovine and *R. rubrum* (Yamaguchi & Hatefi, 1995, 1997; Diggle et al., 1996a).

Figure 3 shows the optical spectra of EcTHSβ1, EcTHSα1, and EcTHSα2. No significant absorbance peaks around 340 nm were found in the spectra for the two purified α domains, suggesting that the reduced substrate, i.e., NADH, was absent in these samples. In the spectrum for EcTHSβ1, a weak absorbance at 340 nm indicated the presence of small amounts of bound NADPH. The maximal absorbance at 267 nm was different from what one might expect from a protein containing four tyrosine residues and one tryptophan. The interpretation of this observation is that substrate is bound to EcTHSβ1. In order to determine the amount of $NADP^+$ and NADPH present in the sample, the optical spectrum was analyzed and compared to protein concentration determinations using the Peterson assay (Peterson, 1977) and the bicinchoninic acid (BCA) method. The theoretical value for the extinction coefficient is 10 810 M^{-1} cm^{-1} (4 Tyr, ϵ = 5120 M^{-1} cm^{-1}; 1 Trp, ϵ = 5690 M^{-1} cm^{-1}) at 280 nm for EcTHSβ1. This value is probably accurate since no absorbance change at this wavelength was observed upon denaturation in 6 M guanidinium chloride (not shown). For a typical preparation, the Peterson method yielded 1.13 mg/mL, and the BCA method 1.33 mg of EcTHSβ1/mL. The calculated [$NADP^+$]/[EcTHSβ1] ratios from these results were 0.73 and 1.35, respectively. Assuming that the [$NADP^+$]/[EcTHSβ1] ratio is 1, and using the extinction coefficient 14 770 M^{-1} cm^{-1} ($\epsilon_{EcTHS\beta1}$ = 10 810 M^{-1} cm^{-1}, ϵ_{NADP+} = 3960 M^{-1} cm^{-1}) at 280 nm, gave a protein concentration of 1.23 mg/mL. From this calculation and the absorbance observed at 340 nm, it is concluded that approximately 95% of EcTHSβ1 contained one bound $NADP^+$ per monomer, and 5% harbored NADPH. To verify the presence of bound $NADP^+$, the strategy described by Diggle and co-workers (Diggle et al., 1996a) was adopted with slight modifications. $NADP^+$ released from EcTHSβ1 was trapped and reduced with isocitrate dehydrogenase (1 unit) and isocitrate (2 mM) in 25 mM sodium phosphate buffer (pH 7.1) containing 5 mM MgCl. The resulting NADPH was measured as a fluorescence increase at 460 nm, using excitation at 340 nm. Comparison of the amount of NADPH produced with protein concentration determined with the bicinchoninic assay suggested approximately 85% occupancy of EcTHSβ1 by $NADP^+$. Diggle and co-workers found that in their domain III preparations from *R. rubrum* both reduced and oxidized substrates were present at approximately 50% each (Diggle et al., 1996a). That EcTHSβ1 was purified in its holoform suggests that the substrate binding affinity is high, that the exchange rate is slow, or both. These questions will be addressed in further detail in the fluorescence section that follows.

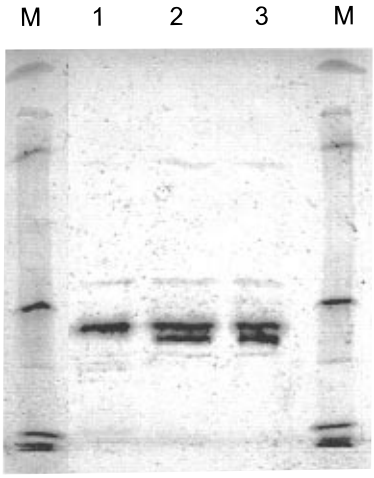

FIGURE 4: Isoelectric focusing gel analysis of EcTHSβ1 in the absence and presence of added substrates. Lane M, low p*I* calibration kit from Pharmacia; lane 1, EcTHSβ1 + 6.7 mM NADPH; lane 2, EcTHSβ1 without addition of substrate; lane 3, EcTHSβ1 + 6.7 mM $NADP^+$. 4 μg of EcTHSβ1 was added to each lane.

Using native isoelectric focusing gels, the isoelectric points for both EcTHSα1 and EcTHSα2 were determined to be about 5.1 (not shown). In both cases, at least two bands were present of which one was ill-defined. This may suggest an inhomogeneity of the soluble α domain population, possibly due to different conformational states. Isoelectric focusing of EcTHSα2 was also performed in the presence of each of the four natural transhydrogenase substrates, i.e., NADH, NAD^+, NADPH, and $NADP^+$. The pattern of bands, however, remained unchanged (not shown). The results from similar experiments with the purified soluble β domain are shown in Figure 4. Two closely positioned bands dominate; their isoelectric points were about 5.7. NADH and NAD^+ had no effect on the band distribution as compared to only EcTHSβ1 (not shown). This was expected since EcTHSβ1 is not supposed to harbor an NAD(H) site. The two dominating bands merged into one band upon

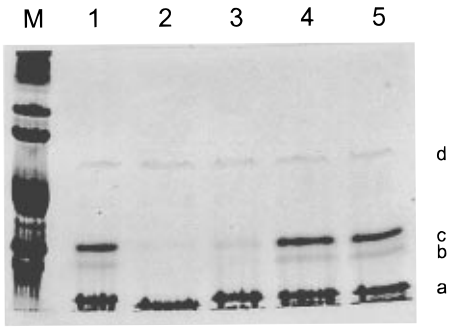

FIGURE 5: Native PAGE analysis of EcTHSβ1 in the absence and presence of added various transhydrogenase substrates. M, low molecular weight markers (see Figure 2); lane 1, purified EcTHSβ1 (same sample as in Figure 2); lane 2, EcTHSβ1 + NADPH; lane 3, EcTHSβ1 + $NADP^+$; lane 4, EcTHSβ1 + NADH; lane 5, EcTHSβ1 + NAD^+; 4 μg of protein was applied to each lane, and each substrate concentration was 6.7 mM. A high-density Phast gel was used in this experiment.

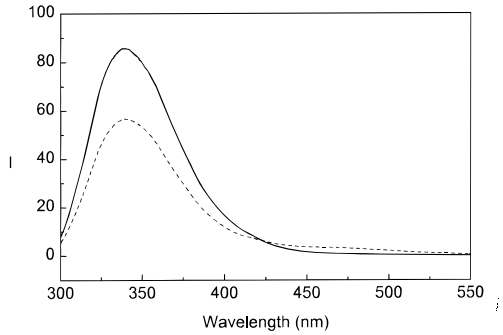

FIGURE 6: Fluorescence emission spectra of EcTHSβ1 in the absence and presence of added NADPH. The solid line represents the emission spectrum of 1.8 μM EcTHSβ1 and the dashed line the spectrum for 1.8 μM EcTHSβ1 and 1.0 μM NADPH. I indicates the relative fluorescence intensity.

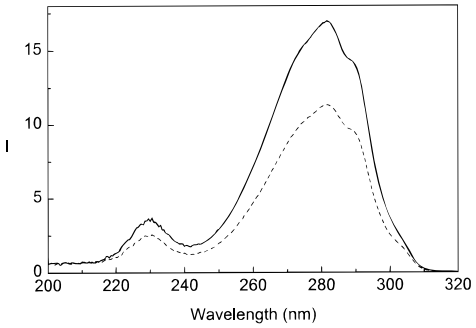

FIGURE 7: Fluorescence excitation spectra of EcTHSβ1 in the absence and presence of added NADPH. The emission wavelength was set at 339 nm where the maximal emission was observed (see Figure 6). The solid line represents the excitation spectrum of 1.8 μM EcTHSβ1 and the dashed line the spectrum for 1.8 μM EcTHSβ1 with 1.0 μM NADPH added. I represents the relative fluorescence intensity.

addition of NADPH. $NADP^+$ did not have any effect, which is consistent with the β domain being purified in its holoform, where $NADP^+$ predominantly occupied the substrate-binding site. Thus, two conformations of the EcTHSβ1·$NADP^+$ complex were present at 15 °C, whereas only one conformation was observed for EcTHSβ1·NADPH.

In order to investigate the conformational changes due to binding of the two substrates, native PAGE gels were run in the presence of each NADH, NAD^+, NADPH, and $NADP^+$. The following points can be made from the results shown in Figure 5: (a) as expected, neither NADH nor NAD^+ had any effect on the band pattern found for the purified EcTHSβ1; (b) in the presence of NADPH, EcTHSβ1 displayed one strong band with a very high electrophoretic mobility; it is likely that this band represents a single tight conformation; (c) high levels of $NADP^+$ also resulted in a partial loss of two bands on the gel, i.e., bands b and c. It was evident from additional native gel runs that higher concentrations of $NADP^+$ than NADPH were required for the disappearance of these two bands. After prolonged storage of EcTHSβ1 at 4 °C, band c disappeared, and band b became progressively stronger which may be due to slow degradation; (d) possibly, EcTHSβ1·NADPH displayed slightly higher electrophoretic mobility than EcTHSβ1·$NADP^+$.

Fluorescence Measurements. A single tryptophan residue is present in position β415 in *E. coli* transhydrogenase. The fluorescence emission spectra in the absence and presence of NADPH are shown in Figure 6. Emission maximum occurred at 339 nm, a slight blue shift from the emission maximum at 349 nm observed for free Trp in water. To determine that the tryptophan indeed was responsible for the observed fluorescence, excitation spectra were collected using 339 nm as the emission wavelength both in the absence and in the presence of added NADPH. As shown in Figure 7, the correlation with the absorbance spectrum for tryptophan is evident, with the characteristic shoulder around 289 nm clearly visible. The small contribution to the emission at 339 nm from the peak centered around 229 nm in the excitation spectrum was not considered. Excitation at 295 nm still yielded a significant emission spectrum (not shown), also supporting that the emission signal mainly arose from the tryptophan residue, and not from tyrosines. Iodide was able to quench all the fluorescence (not shown), which suggests that the Trp residue is accessible to the surrounding medium. However, the side chain is probably not freely rotating in the solvent since maximal emission would then be expected at a value closer to 349 nm.

The tryptophan quenching observed upon addition of NADPH could be a result of conformational changes, energy transfer between the tryptophan residue and NADPH, or a combination of the two. To determine whether resonance energy transfer played a role, emission spectra of NADPH in the presence and absence of EcTHSβ1 were recorded using 280 and 340 nm as excitation wavelengths. The resulting fluorescence emission spectra between 400 and 550 nm are shown in Figure 8. The difference in fluorescence emission between free NADPH and bound NADPH after base line corrections at an excitation at 340 nm was much smaller than that observed when 280 nm was used as the excitation wavelength. Therefore, it is concluded that energy transfer is the major contributor to the tryptophan fluorescence quenching observed upon addition of NADPH. However, the possibility that conformational changes play a role cannot be excluded.

The kinetics of the NADPH-induced tryptophan fluorescence quenching were determined (not shown). It was noted that the background decrease in quantum yield was small (approximately 10%) in comparison to the substrate-induced quenching. After correction for this background, the rate constant for the decay of the fluorescence yield was determined to be about 0.027 s^{-1}. Since EcTHSβ1 contains approximately 95% bound $NADP^+$, this rate constant rep-

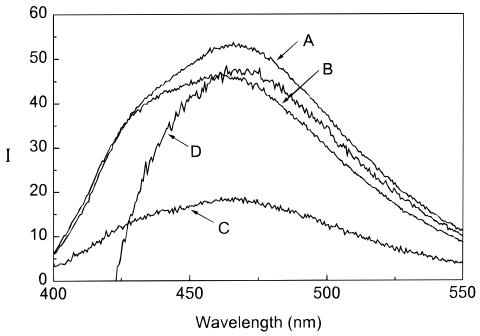

FIGURE 8: Fluorescence emission spectra of NADPH in the absence and presence of added EcTHSβ1. Two spectra were recorded using the excitation wavelength 340 nm, one in the absence of EcTHSβ1 (curve A) and the other in the presence of EcTHSβ1 (curve B). Similarly, two spectra were recorded at the excitation wavelength 280 nm in the absence (curve C) and in the presence (curve D) of EcTHSβ1. The concentrations of EcTHSβ1 and NADPH were 1.8 μM and 1.0 μM, respectively. I indicates the relative fluorescence intensity.

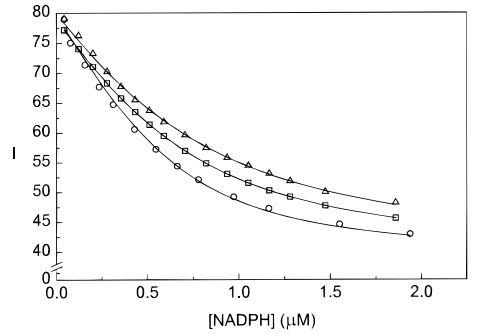

FIGURE 9: Fluorescence quenching of EcTHSβ1 by NADPH. The concentration of EcTHSβ1, calculated by the curve-fitting procedure, was 0.66 μM. Initial fluorescence intensities were normalized to the same values in the three experiments. Other experimental conditions and instrumental settings were as described under Materials and Methods. Fixed concentrations of $NADP^+$ were 6.6 μM (○), 11.3 μM (□), and 17.2 μM (△). Lines represent the smoothed fitted curves assuming simple binding. The curve-fitting procedure is described under Results. I represents the relative fluorescence intensity.

resents $K_{off}^{NADP^+}$ if binding of NADPH is assumed to be fast in comparison to the release of $NADP^+$. The data for NADPH-related fluorescence quenching at various concentrations of $NADP^+$, and the corresponding fitted smoothed curves, are presented in Figure 9 (see Materials and Methods for experimental procedure). The curve-fitting procedure was based on the assumptions that simple binding occurs according to

$$\text{EcTHS}\beta1 + \text{NADPH} \rightleftharpoons \text{EcTHS}\beta1\cdot\text{NADPH}$$

that $NADP^+$ acts as a competitive inhibitor, and that fluorescence intensity is the same for EcTHSβ1 and for the EcTHSβ1·$NADP^+$ complex. In the first step in the curve-fitting procedure, both the EcTHSβ1 concentration and K_d were allowed to vary. Then, the protein concentration was fixed at the average of the three concentrations obtained from the three fitted curves. Thereafter, the curves were refitted, now allowing only for the K_d values to vary. The resulting apparent K_d values derived from curve-fitting were plotted against $NADP^+$ concentration, giving a K_d^{NADPH} of 27 nM and a $K_d^{NADP^+}$ of 1.2 μM (not shown). It should be noted that the results are very sensitive to slight alterations in

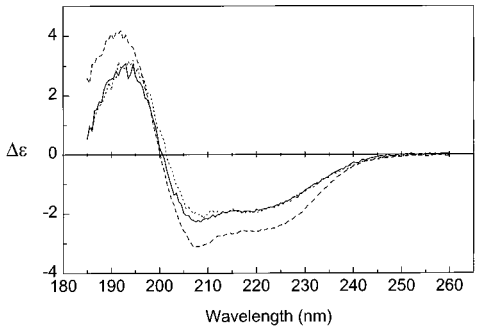

FIGURE 10: CD spectra for EcTHSα1, EcTHSβ1, and EcTHSβ1·NADPH. The dashed line represents EcTHSα1, the solid line EcTHSβ1, and the dotted line EcTHSβ1·NADPH. Conditions were as described under Materials and Methods.

Table 2: Secondary Structure Content of EcTHSα1 and EcTHSβ1[a]

sample	H (%)	AB (%)	PB (%)	T (%)	O (%)
EcTHSα1	27 ± 4	20 ± 4	4 ± 3	19 ± 4	30 ± 4
EcTHSβ1	18 ± 5	26 ± 6	5 ± 3	18 ± 4	31 ± 4

[a] H denotes α-helix; AB, antiparallel β-sheet; PB, parallel β-sheet; T, turn; and O, other structure. The sum of all predicted structures was 100% for each of the domains, EcTHSα1 and EcTHSβ1.

calculated values for protein concentration. However, that $K_d^{NADP^+}$ was approximately 50 times greater than K_d^{NADPH} can be stated with a greater certainty.

The rates of tryptophan fluorescence quenching due to NADPH binding were analyzed at various pH's for estimation of $K_{off}^{NADP^+}$ (data not shown). Varying the amounts of NADPH added, between 13 and 22 molar excess of NADPH over EcTHSβ1, did not alter the kinetics, suggesting that the release rate of $NADP^+$ indeed was rate-limiting. The off rates of $NADP^+$ were determined to be approximately 0.03 and 0.007 s^{-1} at pH 7.1 and 5.8, respectively.

Circular Dichroism Analysis. Circular dichroism is a powerful technique for evaluating the content of various secondary structures in proteins (Johnson, 1990). As seen in Figure 10, both domain I and domain III displayed negative CD bands centered at about 222 and 208 nm, the latter having a more negative amplitude. These bands are indicative of α-helical structures. The overall shapes of the two spectra were similar, but the signal amplitudes were greater for EcTHSα1 than for EcTHSβ1, presumably as a consequence of a greater percentage α-helical structure in the former. Table 2 summarizes the secondary structure content calculated for domains I and III. It was found that EcTHSα1 contains more α-helix than EcTHSβ1, 27 ± 4% versus 18 ± 5%, and less antiparallel β-sheet structure, 20 ± 4% versus 26 ± 6%. Calculations and protein concentration determinations were performed as described under Materials and Methods, with the necessary modifcation to include the contribution from bound $NADP^+$ to the extinction coefficient of EcTHSβ1 at 280 nm (i.e., $\epsilon_{NADP^+} = 3960\ M^{-1}\ cm^{-1} + \epsilon_{EcTHS\beta1} = 10\,810\ M^{-1}\ cm^{-1}$). If this correction was neglected, the calculated α-helical content dropped by about 4%, and the antiparallel β-sheet content increased by about 5%. The results presented here together with previous CD analysis of the intact *E. coli* transhydrogenase (Persson et al., 1991) allowed an estimation of the amount of α-helix in the transhydrogenase portion excluded from the EcTHSα1 and EcTHSβ1 constructions. Using 43% as the value for α-helix content in the wild-type enzyme transhydrogenase

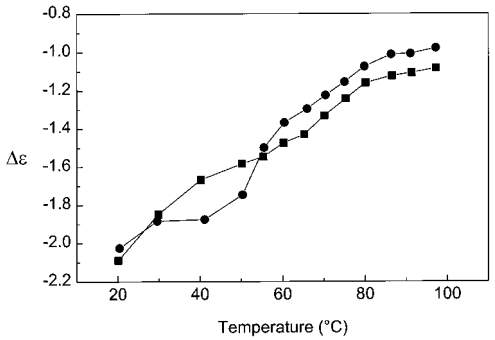

FIGURE 11: Thermal denaturation profiles of EcTHSβ1 in the absence and presence of added NADPH. Symbols denote: (■) without added NADPH; (●) with 43 μM NADPH. At each indicated temperature, the average signal between 213 and 223 nm was plotted (see Figure 12). Other conditions were as described under Materials and Methods.

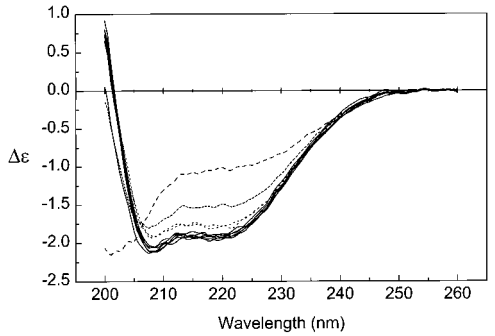

FIGURE 12: CD spectra of EcTHSβ1·NADPH recorded at different temperatures. The spectra were recorded at the following temperatures (in this order): 1, 20.3 °C; 2, 30.3 °C; 3, 20.1 °C; 4, 11.5 °C; 5, 5.8 °C; 6, 45.5 °C; 7, 53.4 °C; 8, 20.3 °C; 9, 88.9 °C; 10, 19.9 °C. Solid lines correspond to spectra 1, 3, 4, 5, 8, and 10. Spectra 2 and 6 are represented by dotted lines, spectrum 7 by a short-dashed line, and spectrum 9 by a dashed line. The concentration of added NADPH was 43 μM. Other conditions were as described under Materials and Methods.

(Persson et al., 1991), and the values for the two individual domains as indicated in Table 2, the 426 residue long nonexpressed portion (essentailly domain II) was calculated to contain approximately 67% α-helix structure. This value is consistent with the notion that the transmembrane-spanning regions are composed of α-helices.

CD spectra were collected for EcTHSα1 in the presence of 50 μM NADH and 50 μM NAD^+, and similarily for EcTHSβ1 in the presence of 50 μM NADPH and 50 μM $NADP^+$. This was done in order to see if structural alterations could be visualized by this technique (not shown, except for NADPH, see Figure 10). For each spectrum, a new base line with the appropriate dinucleotide was recorded and adjusted for. In three of the four experiments, no significant changes of the CD spectra were detected. However, when NADPH was added to EcTHSβ1, a subtle but significant change occurred. A spectrum for EcTHSβ1+NADPH is shown in Figure 10, and the clearest spectral difference was located in the region 195−210 nm, where a 1.5−2 nm shift toward longer wavelengths was observed for the NADPH-bound state of EcTHSβ1. Also, there was a greater difference between the 208 and 222 nm CD signals for EcTHSβ1 without added substrate than for the EcTHSβ1·NADPH complex. Due to the limited sensitivity of the calculation algorithms, the small visual differences shown in Figure 10 do not change the calculated secondary structure content significantly.

Thermal stabilities of EcTHSβ1 and EcTHSβ1·NADPH were investigated. Spectra from 200 to 260 nm were recorded as described under Materials and Methods. In Figure 11, the denaturation profiles for purified EcTHSβ1, i.e., containing about 95% bound $NADP^+$, and EcTHSβ1·NADPH are compared. The small shift in amplitudes between the two curves was probably a result of slight variances in base line correction. What is important though is the relative shape of the curves. The similarity is evident in the region between 60 and 99 °C, whereas at lower temperatures there are distinct differences. Thus, the structure of domain III at temperatures above 60 °C was independent of the substrate being oxidized or reduced. EcTHSβ1·NADPH displayed a plateau between 30 and 40 °C, which indicates one particular conformation. In the case where no substrate was added, no plateau was observed between 20 and 45 °C. It is not possible from these measurements to state whether the EcTHSβ1·$NADP^+$ complex could accommodate different conformations, or if a release of substrate occurred which could have a structural effect. However, the isoelectric focusing results support the former suggestion.

In order to investigate the denaturation behavior further, an additional experiment was performed on the EcTHSβ1·NADPH complex, addressing in particular the reversibility between different conformational states. The resulting CD spectra of this experiment are shown in Figure 12. The spectra displayed as solid lines were collected at approximately 5 and 10 °C, and four spectra at 20 °C. Five of these spectra looked very similar, suggesting that the EcTHSβ1·NADPH complex existed as one conformation at these temperatures, that there was reversibility between the two different holoform conformational states, one observed at 5−20 °C and the other at 30−45 °C, and that there was reversibility after heating the solution to 53 °C. The sixth of these spectra, which was different from the other five, was recorded at 20 °C after the sample had been incubated at 89 °C for more than 20 min. The spectrum crossed the zero line at about 200 nm, the same situation which was observed when no NADPH had been added to the sample. This is to be compared with 201.5 nm at which the CD spectra crossed the zero line in the other five spectra, the situation characteristic for the NADPH-bound form of EcTHSβ1.

DISCUSSION

For the first time, major portions of the extramembranous α-subunit, EcTHSα1 and EcTHSα2, and β-subunit, EcTHSβ1, of *E. coli* transhydrogenase have been overexpressed in the same host, purified, and reconstituted to form catalytically active entities. The specific activities observed for the normal reverse reaction and the cyclic reaction were approximately 200 and 300 times lower, respectively, under the most favorable conditions used here, as compared to the corresponding rates for the intact *E. coli* transhydrogenase. The similar specific activities for EcTHSα1 and EcTHSα2 show that the residues differing in the C-terminals of these constructions are not crucial for catalysis. Domain I exists as a dimer, and there was no evidence for bound substrate, i.e., NAD(H). The purified domain III was found to be momomeric both in the absence and in the presence of NADP(H), and its single substrate-binding site was occupied

by $NADP^+$ (95%) and NADPH (5%). Structural information obtained from CD measurements revealed a greater α-helical content and lower β-sheet content in EcTHSα1 than in EcTHSβ1. Also, the information supported the presumption that domain II is largely composed of transmembrane α-helices. The conformational states of the EcTHSβ1·$NADP^+$ and the EcTHSβ1·NADPH complexes were shown to be significantly different. Substrate-binding studies utilizing the fluorescence properties of the single tryptophan of EcTHSβ1, βTrp415, revealed a 50 times higher affinity for NADPH than for $NADP^+$.

Background of Present Work. In the present investigation, the soluble β-subunit has been kept in focus of attention. In general, the structural information for the NADP(H)-binding site is at present not as detailed as that for the predicted model of the NAD(H)-binding site in the α-subunit (Fjellström et al., 1995). The NADP(H)-binding site constitutes a major portion of the soluble β domain, and it was believed that substrate binding and structural effects due to substrate binding, possibly involved in proton pumping, could be favorably studied in this reduced structure. Rydström and co-workers initially proposed that proton pumping catalyzed by transhydrogenase indeed is mediated by conformational changes in the bovine enzyme (Rydström et al., 1971, 1987; Rydström, 1977). Similar mechanisms were later proposed also for the *E. coli* (Hutton et al., 1994; Hu et al., 1995) and *R. rubrum* enzymes (Diggle et al., 1996a; Yamaguchi & Hatefi, 1997). Subsequently, it was shown by Glavas and co-workers (Glavas et al., 1995) that binding of NADP(H) inflicts conformational changes in the protein, as visualized by changes in exposure of proteolytic sites. Certain mutants of βHis91, e.g., βH91K, are locked in a trypsin-sensitive conformational state, possibly mediated by bound NADP-(H) (Glavas et al., 1995).

Relation between Soluble Domains from Different Species. Domains I and III from *R. rubrum* have previously been characterized (Diggle et al., 1995a,b, 1996a,b) and studied together in reconstituted forms with respect to catalytic properties (Diggle et al., 1996a; Yamaguchi & Hatefi, 1997). Also, the corresponding soluble regions of bovine transhydrogenase have been reconstituted and found to be catalytically active (Yamaguchi & Hatefi, 1997). Multiple sequence alignments indicate only minor differences in length between the various domain I and III constructs (Figure 13). In both *E. coli* domains, histidine tag hexamers have been introduced N-terminally. Yamaguchi and Hatefi (1997) used His-tagged domain III from *R. rubrum*, and it did not seem to hamper catalytic activities. Furthermore, it is unlikely that the lower catalytic activities found here for the reconstituted system in comparison to the wild-type enzyme depend on the N-terminal His-tag in the soluble α domain, since the same His hexamer in the wild-type enzyme did not decrease cyclic reaction rates (unpublished results). Specific activities both for reverse transhydrogenation and for cyclic reaction rates increased as the pH was lowered, in contrast to what Yamaguchi and Hatefi observed (Yamaguchi & Hatefi, 1997).

Binding and Release of NADP(H). It has been observed that lowering the pH causes increased NADP(H) binding in the intact transhydrogenase (Bizouarn et al., 1995), a situation that would stimulate cyclic reaction rates. Therefore, off rates of $NADP^+$ and turnover numbers were investigated at

A

```
E. coli     .......... .......... .......... .......... ..........
bovine   (1) MANLLKTVVT GCSCPFLSNL GSCKVLPGKK NFLRTFHTHR ILWCSAPVKP
R. Rubrum   .......... .......... .......... .......... ..........

E. coli     (α1)  MRIG IPRERLTNET RVAATPKTVE QLLKLGFTVA VESGAGQLAS
bovine      GIPYKQLTVG VPKEIFQNEK RVALSPAGVQ ALVKQGFNVV VESGAGEASK
R. Rubrum   (AA1) MKIA IPKERRPGED RVAISPEVVK KLVGLGFEVI VEQGAGVGAS
                    * *       ***  *  *   *   ** *  ** ***

E. coli     FDDKAFVQAG AEIV..EGNS VWQSEIILKV NAPL...... DDEIALLNPG
bovine      FSDDHYRAAG AQIQ..GAKE VLASDLVVKV RAPMLNPTLG VHEADLLKTS
R. Rubrum   ITDDALTAAG ATIASTAAQA LSQADVVWKV QRPMTAEE.G TDEVALIKEG
              *     ** * *                 **                 *  *

E. coli     TTLVSFIWPA QNPELMQKLA ERNVTVMAMD SVPRISRAQS LDALSSMANI
bovine      GTLISFIYPA QNPDLLNKLS KRKTTVLAMD QVPRVTIAQG YDALSSMANI
R. Rubrum   AVLMCHLGAL TNRPVVEALT KRKITAYAME LMPRISRAQS MDILSSQSNL
              *          *       *   *  *  **    **   ***  * ***  *

E. coli     AGYRAIVEAA .HEFGRFFTG QITAAGKVPP AKVMVIGAGV AGLAAIGAAN
bovine      AGYKAVVLAA .NHFGRFFTG QITAAGKVPP AKILIVGGGV AGLASAGAAK
R. Rubrum   AGYRAVIDGA .YEFARAFPM MMTAAGTVPP ARVLVFGVGV AGLQAIATAK
            *** *    *   ** * *     **** *** *     * ** ***     *

E. coli     SLGAIVRAFD TRPEVKEQVQ SMGAEFLELD ..FKEEAGSG DGYAKVMSDA
bovine      SMGAIVRGFD TRAAALEQFK SLGAEPLEVD ..LKESGEGQ GGYAKEMSKE
R. Rubrum   RLGAVVMATD VRAATKEQVE SLGGKFITVD DEAMKTAETA GGYAKEMGEE
              ** *   *  *    **   * *      *              **** *

E. coli     FIKAEMELFA AQAKEVDIIV TTALIPGKPA PKLITREMVD SMKAGSVIVD
bovine      FIEAEMKLFA QQCKEVDILI STALIPGKKA PILFNKEMIE SMKEGSVVVD
R. Rubrum   FRKKQAEAVL KELVKTDIAI TTALIPGKPA PVLITEEMVT KMKPGSVIID
            *                 **    ******* * * *   **    ** ***  *

E. coli     LAAQN..... ..GGNCEYTV PGEIFTTENG VKVIGYTDLP GRLPTQSSQL
bovine      LAAEA..... ..GGNFETTK PGELY.VHKG ITHIGYTDLP SRMATQASTL
R. Rubrum   LAVEA..... ..GGNCPLSE PGKIV.VKHG VKIVGHTNVP SRVAADASPL
            **           ***      **       *     *    *  *     * *

E. coli     YGTNLVNLLK LLCKEKDG.. .NITVDFD.. ..DVVIRGVT VIRAGEITWP
bovine      YSNNITKLLK AISPDKDNFY FEVKDDFDFG TMGHVIRGTV VMKDGQVIFP
R. Rubrum   FAKNLLNFLT P.HVDKDTKT LVMKLE.... ..DETVSGTC VTRDGAIVHP
              *    *       **                       *   *  *    *

E. coli     AP.PIQVSAQ PQAAQKAAPE VKTEEK (α394)
bovine      APTPKNIPQG APVKQK (410)
R. Rubrum   ALT....GQG A (AA384)
            *
```

B

```
E. coli                       (β286) QEV.G.E HREITAEETA ELLKNSHSVI
bovine                        (860) MEISG.T HTEINLDNAI DMIREANSII
R. rubrum   MNRSIFNVIL GGFGSEGGVA AAGGAAGDRS VKAGSAEDAA FIMKNASKVI
          (B262)                          (B293)                 *

E. coli     ITPGYGMAVA QAQYPVAEIT EKLRARGINV RFGIHPVAGR LPGHMNVLLA
bovine      ITPGYGLCAA KAQYPIADLV KMLSEQGKKV RFGIHPVAGR MPGQLNVLLA
R. rubrum   IVPGYGMAVA QAQHALREMA DVLKKEGVEV SYAIHPVAGR MPGHMNVLLA
            * ****   *  **          *   *  *    *******  **  *****

E. coli     EAKVPYDIVL EMDEINDDFA DTDTVLVIGA NDTVNPAAQD DPKSPIAGMP
bovine      EAGVPYDIVL EMDEINHDFP DTDLVLVIGA NDTVNSAAQE DPNSIIAGMP
R. rubrum   EANVPYDEVF ELEEINSSFQ TADVAFVIGA NDVTNPAAKT DPSSPIYGMP
            **  ***    *  ***       *   **** **  * **   **   * ***

E. coli     VLEVWKAQNV IVFKRSMNTG YAGVQNPLFF KENTHMLFGD AKAS (β462)
bovine      VLEVWKSKQV IVMKRSLGVG YAAVDNPIFY KPNTAMLLGD AKKTCDALQA
R. rubrum   ILDVEKAGTV LFIKRSMASG YAGVENELFF RNNTMMLFGD AKKMTEQIVQ
             * * *   *    ***   * ** * *  *    ** ** ** **

E. coli
bovine      KVRESYQK (1043)
R. rubrum   AMN (B464)
```

FIGURE 13: Multiple sequence alignment of domain I and domain III from *E. coli*, bovine, and *R. rubrum*. The *E. coli* sequences correlate with the domains investigated in the present work, the bovine sequences to the work of Yamaguchi and Hatefi (1997), and the *R. rubrum* sequences to the work of Diggle et al. (1996a) and Yamaguchi and Hatefi (1997). Domain I sequences are shown in (A), and domain III sequences in (B). The alignments have been extracted from a multiple sequence alignment of transhydrogenases from nine different sources, *Escherichia coli*, bovine, mouse, human, *Rhodospirillum rubrum*, *Haemophilus influenzae*, *Eimeria tenella*, *Eimeria acervulina*, and *Entamoeba histolytica*. The GCG package program Pileup was used to create the alignment. In (B), B293 represents the start residue in the domain III construction created by Yamaguchi and Hatefi (1997).

various pHs. At pH 7.1 and 5.8, $K_{off}^{NADP^+}$ was approximately 0.03 and 0.007 s^{-1}, respectively, whereas k_{cat} for the reverse reaction at these pH values was determined to be about 0.009 and 0.023 s^{-1}, respectively. Similar k_{cat} values were determined for the cyclic reaction. These values are curious in several aspects. First, considering the off rate of $NADP^+$, 0.03 s^{-1}, it is odd that EcTHSβ1 is purified in its holoform. In addition, about 95% of the binding sites contained $NADP^+$ and only about 5% NADPH, even though the affinity for NADPH at pH 7.1 is higher than that for $NADP^+$, and at least 90% of the cellular pool of NADP(H) is present in the reduced form (Hoek & Rydström, 1988). Second, at pH 5.7 the off rates and turnover numbers are contradictory for the reverse reaction but not for the cyclic reaction, the off rates being too low. One explanation could be that interactions with domain I, either with or without bound NAD(H), may alter the rate at which $NADP^+$ can depart from domain III. This process may be pH-dependent. However, if the rate-limiting steps are the same for both the reverse and cyclic reactions, i.e., the rate of hydride transfer or the effective concentration of active domain I·III transient complex, then this would explain the parallelled behavior of increased activities at decreased pH.

The observed apparent K_d values for $NADP^+$ and NADPH could be quite different from the corresponding K_d values for the apoenzyme. However, it is clear that the affinity for NADPH is higher than that for $NADP^+$, by a factor of about 50. This result was unexpected since the main function of transhydrogenase probably is to produce NADPH (Hoek & Rydström, 1988). It is proposed that the relative affinities for $NADP^+$ and NADPH can be altered through interactions with the NAD(H)-binding domain of the α-subunit and/or with the membrane-spanning domain II. These postulated affinity changes are likely due to conformational rearrangements which presumably involve binding or release of protons. Diggle and co-workers (Diggle et al., 1995) have shown with one-dimensional NMR techniques that the loop between βC and αD (Fjellström et al., 1995) is mobile when no substrate, i.e., NAD(H), is bound to the α-subunit, and that this mobility is largely lost upon substrate binding. Keeping this in mind, it seems feasable that interactions between domains I and III could differ depending on whether the former is present in its holoform or apoform.

NADP(H)-Dependent Conformational Changes and Proton Pumping. The fact that $NADP^+$ and NADPH trigger the formation of different structural conformations of domain III has important mechanistic consequences. Therefore, there should be residues located close to the nicotinamide ring which are important for the binding affinities for $NADP^+$ and NADPH, and the structural rearrangements caused by substrate binding. Residues Lys-Arg (β424-β425) are suggested to be the most plausible candidates for these purposes. They are conserved in a multiple sequence alignment of 10 different transhydrogenases. The positive charges would explain the higher affinity for the reduced substrate. Conformational alterations could cause a change in the distance between the KR residues and the nicotinamide portion of NADP(H), resulting in an altered affinity for $NADP^+$ relative to that of NADPH.

The conformational changes associated with binding of $NADP^+$ or NADPH are proposed to be conveyed through the protein to affect βHis91, and *vice versa*. This could, for example, cause a pK_a shift of βHis91 to trigger proton translocation events, or to change the accessibility of the βHis91 side chain from one side of the membrane to the other. Reversely, changes in the protonation of βHis91 may then cause the same structural changes in domain III, which are likely to affect the relative affinities for $NADP^+$ and NADPH. These structural changes can be forced upon the system by, for example, mutating βHis91 to a lysine residue. This was demonstrated by Glavas et al. (1995), and changes in substrate affinities were indeed found. Recently, βAsp392 was found to be important for both catalytic and proton-pumping activity, and it has been proposed to participate as a link in a proton translocation pathway (Meuller et al., 1996). It is possible that protonation of this aspartate residue in the reconstituted system investigated here could have a role in the higher catalytic activities observed at lower pH.

In conclusion, conformational states of domain III in *E. coli* transhydrogenase are dependent on whether it contains bound $NADP^+$ or bound NADPH. EcTHSβ1·NADPH could adopt two distinct conformations as judged by CD. Also, EcTHSβ1·$NADP^+$ could exist in at least two forms. Substrate affinities are likely to be affected by these structural changes. Since a mixture of domain I and domain III was found to be catalytically active, it is suggested that the conformational and mechanistic studies of the isolated domain III are relevant to the intact enzyme as well.

ACKNOWLEDGMENT

We are grateful to Dr. Lars-Erik Andreasson and Dr. Mikael Kubista for advice concerning fluorescence measurements. We also thank Ann-Cathrine Smiderot for help with protein purification.

REFERENCES

Ahmad, S., Glavas, N. A., & Bragg, P. D. (1992) *Eur. J. Biochem. 207*, 733−739.

Bizouarn, T., Grimley, R. L., Cotton, N. P. J., Stillwell, S. N., Hutton, M., Jackson, J. B. (1995) *Biochim. Biophys. Acta 1229*, 49−58.

Bizouarn, T., Diggle, C., Quirk, P. G., Grimley, R. L., Cotton, N. P., Thomas, C. M., & Jackson, J. B. (1996a) *J. Biol. Chem. 271*, 10103−10108.

Bizouarn, T., Diggle, C., & Jackson, J. B. (1996b) *Eur. J. Biochem. 239*, 737−741.

Clarke, D. M., & Bragg, P. D. (1985) *J. Bacteriol. 162*, 367−373.

Diggle, C., Hutton, M., Jones, G. R., Thomas, C. M., & Jackson, J. B. (1995a) *Eur. J. Biochem. 228*, 719−726.

Diggle, C., Cotton, N. P., Grimley, R. L., Quirk, P. G., Thomas, C. M., & Jackson, J.B. (1995b) *Eur. J. Biochem. 232*, 315−326.

Diggle, C., Bizouarn, T., Cotton, N. P. J., & Jackson, J. B. (1996a) *Eur. J. Biochem. 241*, 162−170.

Diggle, C., Quirk, P. G., Bizouarn, T., Grimley, R. I., Cotton, N. P., Thomas, C. M., & Jackson, J. B. (1996b) *J. Biol. Chem. 271*, 10109−10115.

Fjellström, O., Olausson, T., Hu, X., Källebring, B., Ahmad, S., Bragg, P. D., & Rydström, J. (1995) *Proteins: Struct., Funct., Genet. 21*, 91−104.

Genetics Computer Group (1991) *Program Manual for the Wisconsin Package*, Version 8, September 1994, Genetics Computer Group, 575. Science Dr., Madison, WI 53711.

Glavas, N. A., & Bragg, P. D. (1995) *Biochim. Biophys. Acta 1231*, 297−303.

Glavas, N. A., Hou, C., & Bragg, P. D. (1995) *Biochemistry 34*, 7694−7702.

Hennessey, J. P., Jr., & Johnson, W. C., Jr. (1981) *Biochemistry 20*, 1085−1094.

Hoek, J. B., & Rydström, J. (1988) *Biochem. J. 254*, 1−10.
Holmberg, E., Olausson, T., Hultman, T., Rydström, J., Ahmad, S., Glavas, N. A., & Bragg, P. D. (1994) *Biochemistry 33*, 7691−7700.
Hu, H., Zhang, J., Persson, A., & Rydström, J. (1995) *Biochim. Biophys. Acta 1229*, 64−72.
Hutton, M., Day, J. D., Bizouarn, T., & Jackson, J. B. (1994) Eur. J. Biochem. *219*, 1041−1051.
Jackson, J. B. (1991) *J. Bioenerg. Biomembr. 23*, 715−741.
Johnson, W. C., Jr. (1990) *Proteins: Struct., Funct., Genet. 7*, 205−214.
Kubista, M., Sjöback, R., Eriksson, S., & Albinsson, B. (1994) *Analyst 119*, 417−419.
Laemmli, U. K. (1970) *Nature 227*, 680−685.
Meuller, J., Hu, X., Bunthof, C., Olausson, T., & Rydström, J. (1996) *Biochim. Biophys. Acta 1273*, 191−194.
Meuller, J., Hou, C., Bragg, P. D., & Rydström, J. (1997) *Biochem. J. 324*, 681−687.
Olausson, T., Fjellström, O., Meuller, J., & Rydström, J. (1995) *Biochim. Biophys. Acta 1231*, 1−19.
Palmer, T., & Jackson, J. B. (1992) *Biochim. Biophys. Acta* 1099, 157−162.
Persson, B., Rydström, J., & Kubista, M. (1991) *Biophys. Chem. 39*, 267−272.
Peterson, G. L. (1977) *Anal. Biochem. 83*, 346−356.
Rost, B., & Sander, C. J. (1993) *J. Mol. Biol. 232*, 584−599.
Rost, B., Sander, C., & Schneider, R. (1994) *CABIOS 10*, 53−60.
Rydström, J. (1977) *Biochim. Biophys. Acta 463*, 155−184.
Rydström, J., Teixeira da Cruz, A., & Ernster, L. (1971) *Eur. J. Biochem. 23*, 212−219
Rydström, J., Persson, B., & Carlenor, E. (1987) in *Pyridine Nucleotide Coenzymes: Chemical, Biochemical & Medical Aspects* (Dolphin, D., Poulson, R., & Avramovic, O., Eds.) Vol. 2B, pp 433−460, John Wiley & Sons, Inc., New York.
Weisberg, S. (1985) *Applied Linear Regression*, pp 203−223, Wiley, New York.
Williams, R., Cotton, N. P., Thomas, C. M., & Jackson, J. B. (1994) *Microbiology 140*, 1595−1604.
Wittung, P., Källebring, B., & Malmström, B. G. (1994) *FEBS Lett.*, 286−288.
Yamaguchi, M., & Hatefi, Y. (1994) *J. Bioenerg. Biomembr. 26*, 435−445.
Yamaguchi, M., & Hatefi, Y. (1995) *J. Biol. Chem. 270*, 28165−28168.
Yamaguchi, M., & Hatefi, Y. (1997) *Biochim. Biophys. Acta 1318*, 225−234.
Zhang, J., Hu, X., Osman, A.-M., & Rydström, J. (1997) *Biochim. Biophys. Acta 1319*, 331−339.

BI970958F